ISSN 2321-807X

Synthesis, Crystal Structure and Vibrational Properties of bis (N-benzylmethylammonium) Pentachlorobismuthate (III).

Hiba Khili[a], Najla Chaari[a], Mohamed Fliyou[b], Slaheddine Chaabouni[a].

[a] Laboratoire des Sciences des Matériaux et de l'Environnement, département de chimie, Faculté des Sciences de Sfax, BP 1171, 3018 Sfax, Tunisia.

E-mail address: Kh.Hiba@hotmail.com; n_chaari2003@yahoo.fr; chaabouni_slaheddine@yahoo.fr.

[b] ENS de Marrakech, Département de physique, Université Cadi-Ayyad Marrakech, Morocco.

E-mail address: fliyou@hotmail.com.

Abstract

The $[C_8H_{12}N]_2$ $BiCl_5$ compound crystallised in the triclinic system with space group P^{-1} with *a* = 9,833(4), *b* = 10,044(7), *c* = 12,225(7) Å, α= 78.82(4), *β* = 75,42(4), γ= 76.89°(5) and Z = 2. The average density value, ρ_x = 1.518 $g.cm^{-3}$ is in agreement with the calculated one, ρ_x = 1.494 $g.cm^{-3}$. The atomic arrangement can be described as an alternation of organic and inorganic layers. The anionic layer is built up of octahedral $[Bi_2Cl_{10}]^{-4}$. The organic layers are arranged in sandwich between the anionic ones. The crystal packing is governed by means of the ionic N–H---Cl hydrogen bonds, forming a three dimensional network. The nature of the distortion of the inorganic polyhedra has been studied and can be attributed to the stereo activity of the Bi(III) lone electron pair. The infrared and Raman spectra was recorded in the 4000–400 cm^{-1} frequency region.

Keywords: Organic–inorganic hybrid material; Decachlorodibismuthates(III); Halogenobismuthates(III); Phase transition; IR absorption; Raman scattering.

***Corresponding author:** Hiba Khili**.**

Tel: +21698813420, **fax** +21674274437

E-mail address: kh.hiba@hotmail.com

Address: Route de Soukra km 3.5 - B.P. n° 1171 - 3000 Sfax.

Council for Innovative Research

Peer Review Research Publishing System

Journal: Journal of Advances in Chemistry

Vol. 8, No. 2

editor@cirworld.com

www.cirjac.com, member.cirworld.com

ISSN 2321-807X

I. Introduction

Recently, a great attention has been focused on organic-inorganic hybrid materials based on metal-halide units; those materials are frequently characterized by their various physical and chemical properties that could lead to technological innovations like magnetic or ferroelectric transitions, conductivity (super conductivity), electroluminescence, and photoluminescence [1-6].

The alkylammonium halogenoantimonates(III) and bismuthates(III) of the general formula $R_aM_bX_{3b+a}$ (where R denotes organic cations, M= Sb, Bi and X = Cl, Br, I) evoke much interest because of their ferroelectric and ferroelastic properties [7–9]. Numerous compounds of this family display frequently multiple structural phase transitions [10, 11].

To date, numerous metal–halide systems involving Bi and Sb have been synthesized and structurally characterized [6,12–19]. The anionic metal–halide species has been observed to range in dimensionality from two-dimensional or one-dimensional polymeric anions to discrete anions of various sizes.

The bismuth compounds represent a potential class of materials with unusual structural arche- types, due to the fact that the Bi(III) ion exhibits a variety of coordination mode, depending on crystal packing and on ligands: octahedral coordination being observed.

The structural chemistry of bismuth halides in the solid state form various structures [12, 14, 6], mainly with an anionic sublattice built-up of the MX_6 octahedra sharing corners, edges or faces into numerous different arrangements leading to an extensive family of bismuth(III) halogenoanions ($[BiX_4]^-$, $[BiX_5]^{2-}$, $[BiX_6]^{3-}$, $[Bi_2X_9]^{3-}$, $[Bi_2X_{10}]^{4-}$, $[Bi_2X_{11}]^{5-}$, $[Bi_3X_{12}]^{3-}$, $[Bi_4X_{18}]^{6-}$, $[Bi_6X_{22}]^{4-}$, and $[Bi_8X_{30}]^{4-}$) [20–27]. Structure of the anionic form is related to the size and symmetry of the organic counterions and their ability to form hydrogen bonds as well.

In fact, as well as the rich structural diversity displayed by these systems, some interest has been directed towards halobismuthate(III) compounds in combination with organic cations, due to their very interesting physical properties caused by active lone pairs [28]. The main types of transitions have been governed by the displacement dynamics of the ammonuim cations [17, 19]. It is associated with changes in the hydrogen bonding joining the organic–inorganic chains.

We have successfully synthesized a new compound of formula $[C_8H_{12}N)_2]$ $BiCl_5$. In the present paper, we report the synthesis, the structural characterizations by X-ray diffraction, the differential scanning calorimetry (DSC) and vibrational studies of the bis (N-benzylmethylammonium) pentachlorobismuthate (III).

II. Experimental section

II.1. General

All reagents were purchased commercially and used further purification. The X-ray data-collections were carried out on Bruker APEXII CCD four circle diffractometer using Mo Kα radiation. The DSC measurements were recorded on a NETZSCH apparatus (Model 204 Phoenix) with the heating/cooling rates at a heating rate of 5 $K.min^{-1}$. The infrared (IR) spectra were recorded in the 4000–400 cm^{-1} region by using KBr pellet on a Nicolet Impact 410 spectrometer.

Raman spectra were measured with a LABRAMHR 800 triple monochromator. The spectra slit widths were set to maintain a resolution of approximately 3 cm^{-1}. The excitation light was 632.81nm line of He-Ne (20mV) ion laser. Measurements were carried under microscope in an open furnace (under air, at ambient pressure) at room temperature for the first compound and on heating from 298 to 428 K for the second. The heating rate is 10 K/min, waiting for 1 min after stabilisation of temperature and collecting time for each spectrum is 10 seconds.

II.2. Synthesis

The $[C_8H_{12}N]_2BiCl_5$ crystals were prepared by dissolving bismuth(III) nitrate and the correspondent cation in concentrated HCl solution in stoichiometric ratio. The reaction occurs in the presence of ethanol (50 ml) and water (20 ml). The resulting aqueous solution is then kept at room temperature. After slow evaporation, parallelepipedic monocrystals appeared in the solution. Density was measured at room temperature by flotation in CCl4. Intensities data were collected using a Bruker APEXII CCD four circle diffractometer with graphite- monochromated (Mo Ka). The positional parameters for the heavy atoms were obtained from a three-dimensional Patterson map, while the non-H atoms were found from successive difference Fourier Maps. The structure is refined by full-matrix least squares using anisotropic temperature factors for all non-hydrogen atoms, the hydrogen atoms were localized and optimized to restraint positions. Calculations were performed with the SHELXS-86 program [29], using the scattering factors inclosed therein. Crystal data, collected reflections and parameters of final refinement are reported in Table 1.

ISSN 2321-807X

Table 1. Crystal data and summary of intensity data collection and structure refinement.

Compound	$[C_8H_{12}N]_2\ BiCl_5$
Molecular weight	315,31
Color/Shape	yellow / Parallelepipedic
System	Triclinic
Space group	P^{-1}
Temperature (K)	296(2)
Cell constants	
a, Å	9.8330(4)
b, Å	10.0440(7)
c, Å	12.2250(7)
α, °	78.820(4)
β, °	75.420(4)
γ, °	76.898(5)
Cell volume, $Å^3$	1126.02(1)
Formula units/ unit cell	2
$D_{calc.}$	1.860
Diffractometer/scan	Bruker APEXII CCD Diffractometer
Radiation, graphite monochromator	Mo K_α (λ= 0.7107 Å)
Max. crystal dimensions, mm	0.28 x 0.16 x 0.10
$\mu_{calc.}$, mm^{-1}	8.424
Unique Reflections	8359
θ range, deg	$3.070 \leq \theta \leq 33.99$
Reflections with $I > 4\sigma(F_o)$	3598
Range of h, k, l	-15/14, -15/15, -19/18
F(000)	604
Weights	$w = 1/[\sigma^2(F_o^2)+(0.0326\ P)^2]$ where $P = Max[(F_o^2, O) + 2F_c^2]/3$
$R = \sum\|\|F_o\| - \|F_c\|\| / \sum\|F_o\|$	0.0315
wR =	0.0273
Goodness-of-fit (GOF) = S	1.1264

III. Results and discussion

III.1. Crystallographic study

The final atomic coordinates obtained from the single crystal refinement with Ueq are given in Table 2. Interatomic distances, bond angles and hydrogen bonds schemes are listed in Table 3. The Bi atoms are surrounded by six Cl^- ions in a distorted octahedral arrangement. Two chlorine atoms bridge nearly symmetrically the two metals. The asymmetric unit of **$[C_8H_{12}N]_2\ BiCl_5$** is made up of half of the dimeric decachlorodibismuthate(III) which has the geometry of two octahedra sharing one edge, and two independent 4-benzylpyridinium cations (Figure 1).

ISSN 2321-807X

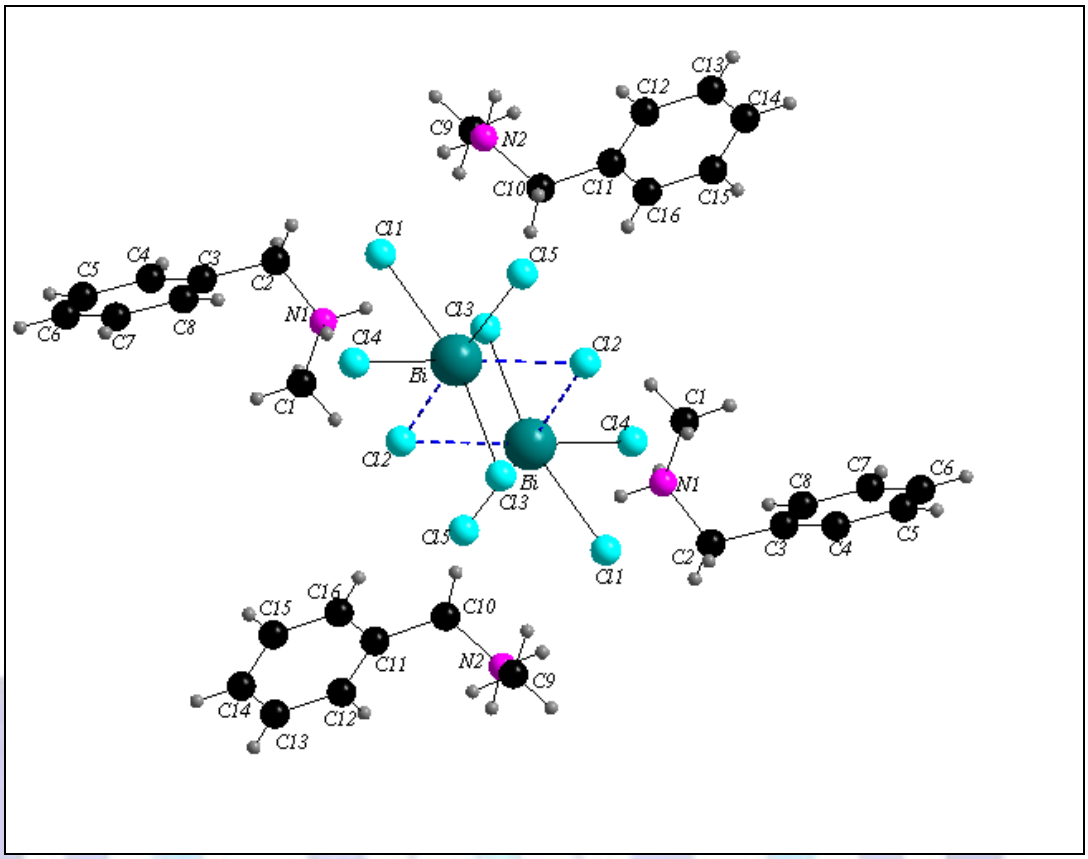

Fig 1: Atom numbering scheme for the title compound $[C_8H_{12}N]_2\,BiCl_5$.

The spaces between the inorganic entities are filled by organic cations assuring their connection by means of the N–H- - -Cl hydrogen bonds, forming a three-dimensional network. The nature of the distortion of the $[BiCl_6]^{3-}$ polyhedra has been studied and can be attributed to the stereo activity of the Bi(III) lone electron pair (ID (Bi–Cl)= 3,174 10^{-3} %) . A perspective view of **$[C_8H_{12}N]_2\,BiCl_5$** (Figure 2) shows that the bioctaèdres $[Bi_2Cl_{10}]^{4-}$ are arranged parallel to the axis b and pass through the center of the planes (a, c) at x = 1/2 and z = 1 / 2. The structure of the projection in the plane (b, c) shows an alternation of the orientations of cationic group arranged parallel to the axis b (Figure 3).

The distorted octahedral chlorine coordination around bismuth is characterized by a range of Bi–Cl bond lengths from 2,573 (1) to 2,952 (1) Å (Table 3) and an average bond length of 2,735 (1) Å. Cl– Bi–Cl bond angles range from 83,17(5) to 102,63(5)° for cis and from 166,90(5) to 172,30(5)° for trans arrangements. In addition to the bond length differences, the Cl–Bi–Cl bond angles (Table 3) deviate substantially from 90°, with the biggest difference [96,83(6)°] occurring for the Cl(3)–Bi–Cl(5) angle, which incorporates the two shortest Bi–Cl bonds. The distortion of the $[Bi_2Cl_{10}]^{4-}$ octahedra is correlated both to primary deformations resulting from the stereochemical activity of Bi lone electron pair [28,30] and to secondary deformations resulting from hydrogen bond interactions [31]. The involvement of any particular chlorine atom in hydrogen bonding brings about the shift of the lone electron pair of Bi atom in the direction of H atom, which generally results in the shift of the respective Cl atom out of the Bi position. This leads to the increase in the Bi–Cl bond length of terminal (Bi–Cl) (2.909 Å).

ISSN 2321-807X

Table 2. Atomic coordinates and U_{eq} or U_{iso} for $[C_8H_{12}N]_2$ $BiCl_5$ and $[C_{12}H_{12}N)_2]$ $BiCl_5$.

Atoms	x/a	y/b	z/c	U_{eq}[a]
Bi1	0,63491(3)	0,80604(3)	0,54986(2)	0,0268
Cl1	0,41389(2)	0,65808(2)	0,60871(1)	0,0423
Cl2	0,57917(2)	0,98829(2)	0,33914(1)	0,0421
Cl3	0,83485(2)	0,94848(2)	0,54430(1)	0,0499
Cl4	0,71924(2)	0,64792(2)	0,72195(1)	0,0461
Cl5	0,79297(2)	0,63565(2)	0,41499(1)	0,0493
N1	0,8800(7)	1,1168(7)	0,2885(5)	0,0547
C1	0,9438(9)	0,9948(1)	0,2303(8)	0,0723
C2	0,9526(9)	1,2380(9)	0,2442(6)	0,0592
C3	0,9683(7)	1,2785(7)	0,1188(6)	0,0448
C4	1,0993(8)	1,2625(1)	0,0447(7)	0,0653
C5	1,1150(1)	1,2973(1)	-0,0715(8)	0,084
C6	0,9964(1)	1,3515(1)	-0,1159(7)	0,0687
C7	0,8640(1)	1,3674(1)	-0,0446(7)	0,0761
C8	0,8504(8)	1,3312(1)	0,0715(7)	0,0636
N2	0,6805(6)	0,3800(5)	0,6174(4)	0,0437
C9	0,8314(8)	0,3191(8)	0,6135(7)	0,055
C10	0,5775(8)	0,2855(7)	0,6792(6)	0,0483
C11	0,5725(7)	0,2533(7)	0,8044(5)	0,0421
C12	0,4987(8)	0,3497(8)	0,8762(6)	0,0553
C13	0,4895(1)	0,3189(9)	0,9930(7)	0,0669
C14	0,5544(1)	0,1941(1)	1,0390(7)	0,0741
C15	0,6278(1)	0,0958(1)	0,9691(8)	0,0728
C16	0,6350(1)	0,1259(9)	0,8534(7)	0,0611

$U_{éq} = 1/3 \sum_i \sum_j U_{ij}\, a_i\, a_j\, a_i^*\, a_j^*$

The C=C bond length vary from 1.366(1) to 1.378(1).The C–C and C-N bond length vary from 1.472(1) to 1.493(1) Å. The rings of the successive cations are approximately parallel to each other and equidistant (Figure 3): the adjacent aromatic rings are separated by centroid-to-centroid distances varying from 8,131(2) to 8,778 (2) Å, which are too large to be considered as representing π–π stacking interactions [32]. In the title compound, the rings built up by the atoms (C3, C4, C5, C6, C7, C8) and (C11, C12, C13, C14, C15, C16) are planar (rms deviation of fitted atoms equal to 0,0044 and 0,0065, respectively).

ISSN 2321-807X

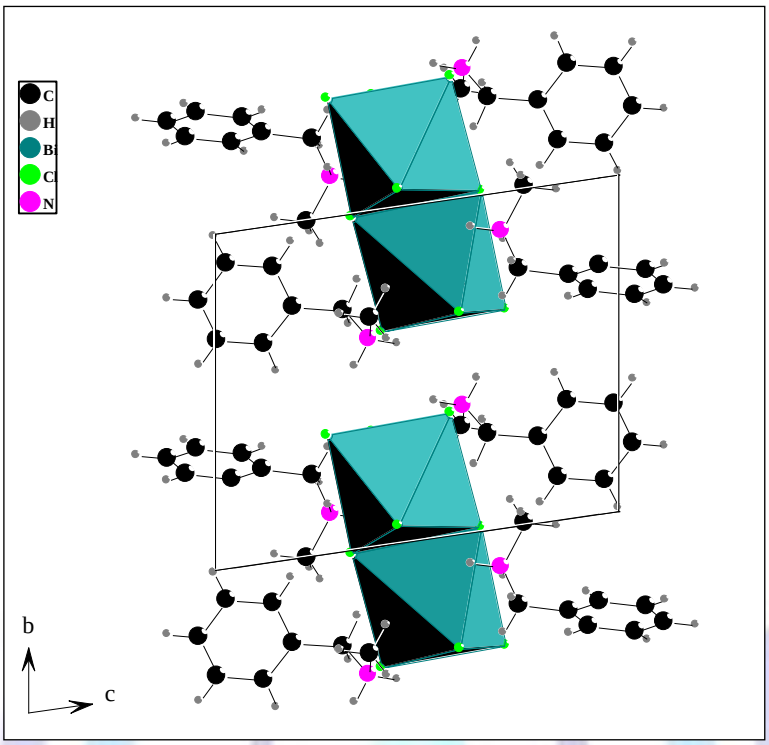

Fig 3: Projection in the plane (b,c) of the atomic arrangement of $[C_8H_{12}N]_2\,BiCl_5$.

In **$[C_8H_{12}N]_2\,BiCl_5$**, the organic species interact with the inorganic chains via N–H---Cl hydrogen bonds (Table 3)(figure 3); there are seven weak N–H---Cl hydrogen bonds [33].

Table 3. Principal intermolecular distances (Å) and angles (°) in $[C_8H_{12}N]_2\,BiCl_5$.

Bond lengths and angles			
Bi-Cl1	2.777(1)	N1-C1	1.472(12)
Bi-Cl2	2.952(1)	C2-N1	1.493(10)
Bi-Cl3	2.662(1)	C3-C2	1.486(10)
Bi-Cl4	2.573(1)	C4-C3	1.372(11)
Bi-Cl5	2.581(2)	C5-C4	1.373(13)
Bi-Cl2[a]	2.867(2)	C6-C5	1.366(15)
		C6-C7	1.367(13)
		C7-C8	1.374(11)
		C8-C3	1.378(10)
		N2-C9	1.463(10)
		C10-N2	1.507(8)
		C11-C10	1.493(9)
		C12-C11	1.387(10)
		C13-C12	1.385(11)
		C14-C13	1.356(13)
		C15-C14	1.385(15)
		C15-C16	1.375(12)
		C16-C11	1.380(11)
Cl1-Bi-Cl2	102.63(5)	C2-N1-C1	115.2(6)

Cl1-Bi-Cl3	166.97(5)	N1-C2-C3	112.3(6)
Cl1-Bi-Cl4	84.01(5)	C2-C3-C4	122.0(7)
Cl1-Bi-Cl5	92.25(5)	C3-C4-C5	122.5(8)
Cl1-Bi-Cl2[a]	83.17(5)	C4-C5-C6	119.3(8)
Cl2-Bi-Cl3	87.44(5)	C5-C6-C7	119.7(7)
Cl2-Bi-Cl4	172.30(5)	C2-C3-C8	121.1(7)
Cl2-Bi-Cl5	85.41(5)	C4-C3-C8	116.9(7)
Cl2-Bi-Cl2[a]	83.64(5)	C3-C8-C7	121.4(7)
Cl3-Bi-Cl4	86.59(5)	C8-C7-C6	120.2(8)
Cl3-Bi-Cl5	96.83(6)	C10-N2-C9	114.7(5)
Cl3-Bi-Cl2[a]	89.85(6)	N2-C10-C11	112.7(5)
Cl4-Bi-Cl5	90.47(6)	C10-C11-C12	120.5(6)
Cl4-Bi-Cl2[a]	87.77(2)	C11-C12-C13	120.9(7)
Cl5-Bi-Cl2[a]	166.90(5)	C12-C13-C14	120.4(8)
		C15-C14-C13	119.8(8)
		C16-C15-C14	119.7(9)
		C10-C11-C16	121.7(7)
		C12-C11-C16	117.8(6)
		C11-C16-C15	121.4(8)

Hydrogen bonds

D-H…A	*d(D-H) (Å)*	*d(H...A) (Å)*	*d(D...A) (Å)*	*<DHA (°)*
N1-H1.1…Cl2	0.9	2.725	3.36(1)	128.51(5)
N1-H1.1…Cl1	0.9	2.756	3.369(1)	126.45(4)
N1-H1.2…Cl3	0.9	2.395	3.228(9)	154.13(4)
N2-H2.1…Cl4	0.9	2.5	3.328(8)	153.25(3)
N2-H2.1…Cl1	0.9	2.86	3.375(1)	117.8(3)
N2-H2.2…Cl1	0.9	2.472	3.242(7)	143.69(3)
N2-H2.2…Cl5	0.9	2.861	3.375(1)	117.74(3)

symmetry code= [a] = -x+1. -y+2. -z+1

ISSN 2321-807X

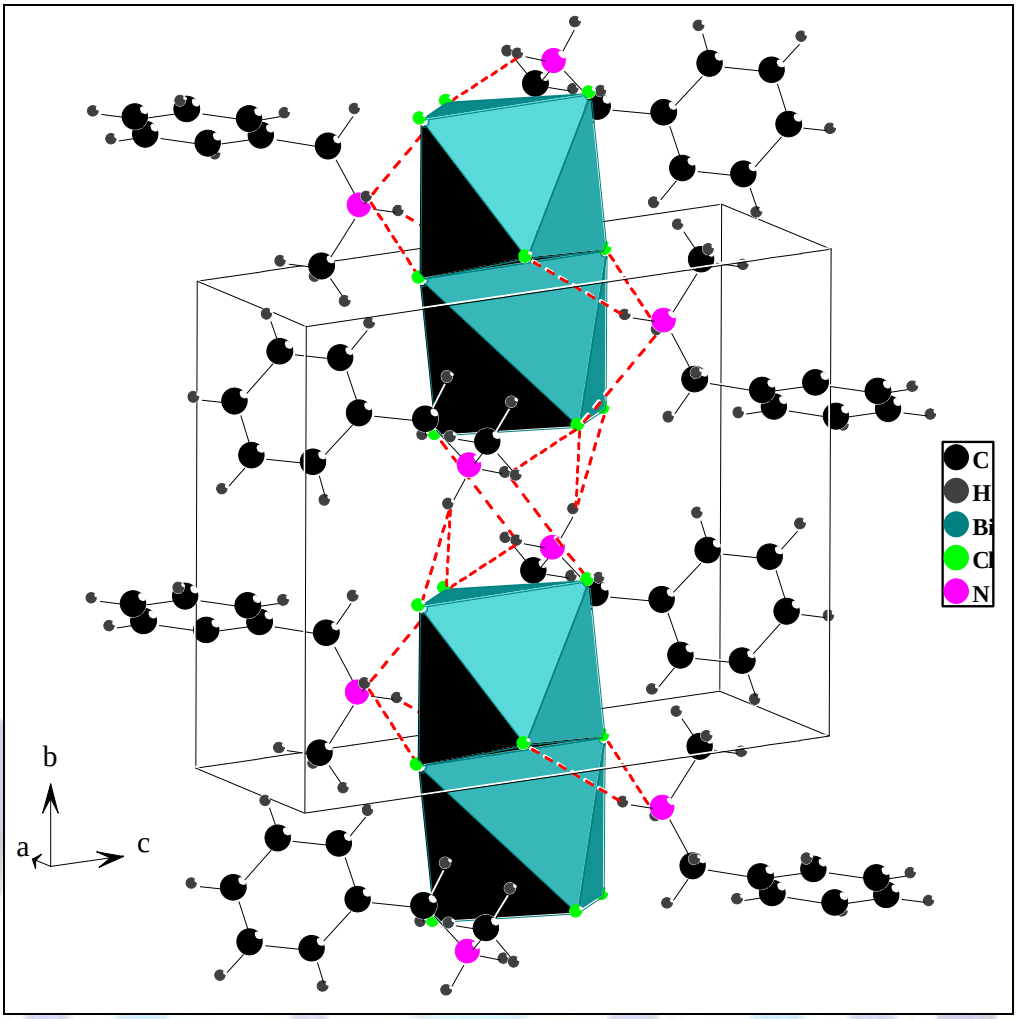

Fig 3: Perspective view of $[C_8H_{12}N]_2\,BiCl_5$ and N–H…Cl hydrogen bonds (dashed lines).

III.2. Calorimetric study

A typical result of the calorimetric study of this compound is presented in Figure 4 which shows the diagram obtained by heating the sample from 290 K to 470 K. Two distinct endothermic peaks were detected at 407 K and 420 K (heating). The last one corresponds to the melting of the product whereas the first denotes a structural phase transition; from the phase I to phase II; which is clearly of first-order type. Taking into account that the anionic sublattice in this salt is composed of large polyanionic unit. the N-Benzylmethylammonium cation seems to contribute to the mechanism of the phase transition [4,5].

ISSN 2321-807X

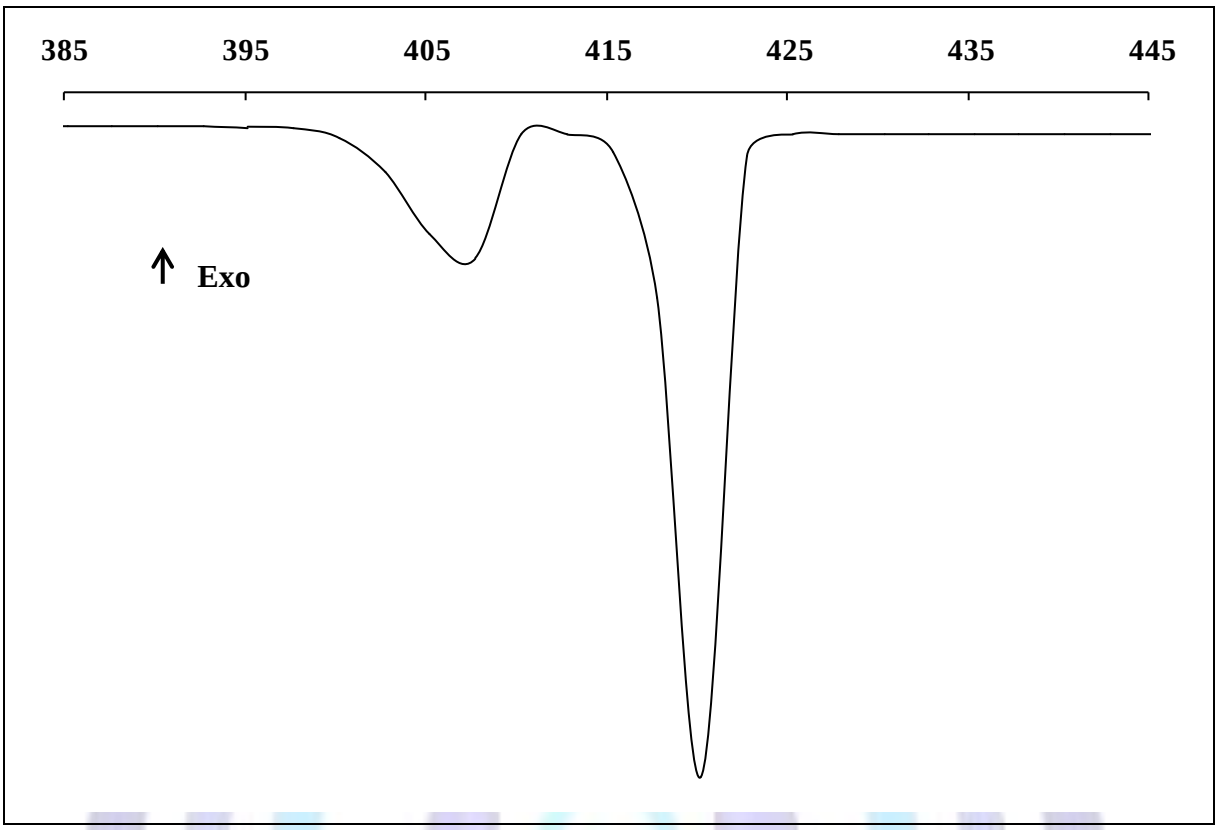

Fig 4: Differential scanning calorimetry curve of $[C_8H_{12}N]_2BiCl_5$.

III.3. Vibrational studies

To gain more information on the crystal structure, we have undertaken a vibrational study using infrared spectroscopy and Raman scattering. The tentative assignments of the vibrations are based on a comparison of the infrared and Raman spectra of **$[C_8H_{12}N]_2BiCl_5$** with other spectra known from the literature about numerous chlorobismuthate(III) compounds [34–39]. The vibrational studies have been undertaken to obtain further information on the dynamics of the organic cations, especially on the disorder degree of these cations in different phases and their contribution to the phase transitions mechanism. The Raman and infrared peaks frequencies are quoted in Table 4. The IR and Raman spectra of **$[C_8H_{12}N]_2BiCl_5$** (Figure 6) were recorded for the wavenumber region between 4000 and 400 cm^{-1}.

III.3.1. External modes

By comparison with previous works reported on similar compounds containing $[BiCl_5]$ we may propose a tentative assignment of the observed bands [32, 34]. In figure 5, for the dimeric decachlorodibismuthate(III) tetraanions the Bi–Cl external symmetric stretching vibration is seen to give rise to the strongest Raman lines at 260 and 269 cm^{-1}.

The 230 and 218 cm^{-1} band arises from the Bi–Cl external symmetric and antisymmetric stretching. Raman lines at 157 and 156 and cm^{-1} most likely correspond to the Cl–Bi–Cl stretch. Frequencies for the bending modes occur near 106 cm^{-1}. The lattice modes can be observed in the Raman spectra between 78 and 54 cm^{-1}.

III.3.2. Internal modes [35, 36, 37, 38]

The infrared and Raman spectra of the title compound $[C_8H_{12}N]_2$ $BiCl_5$ shows the bonds corresponding to vibrations of N-benzylmethylammonium cations (figure 6). The assignment of the internal modes of the organic cations is based on the comparison with the well-documented spectra of the homologous compounds [35- 38]. The IR spectra shows at high wavenumbers an absorption centered at 3461 cm^{-1} assignable to ν(N-H) of the secondary amine. The asymmetric and the symmetric bending vibration of (NH_2^+) and (C–H) aromatic appears respectively at 3134 and 3081 cm^{-1}; these two bands are observed in Raman spectra respectively at 3106 and 3088 cm^{-1}. The broad absorption bands in the 2808–3020 cm^{-1} range correspond to $\nu(CH_2)$ whereas the band at 2719 cm^{-1} is assigned to $\nu(CH_3)$. The bands observed at 2436 and 2339 cm^{-1} can be assigned to $\delta(NH_2^+)$ which are not detected in Raman spectra. In IR spectra, the bands at 1497 and 1577 cm^{-1} associated with the ν(C=C) of the aromatic ring are observed in Raman spectra at 1561–1581 cm^{-1}.

The absorption band located at 1456 cm^{-1} corresponds to $\delta(CH_3)$ band and the deformation of the (N–H) band. The vibrations at 1405 cm^{-1} is due to $\delta(CH_2)$ and ν(C–H) aromatic and that at 1383 cm^{-1} to the deformation of (C–H)

aromatic. The bands with frequency at 1325 and 1383 cm^{-1} are ascribed for the $\omega(CH_2)$ and the deformation of (C–H) aromatic. The band at 1267 cm^{-1} is caused by $\tau(CH_2)$ and that at 1212 cm^{-1} by λ(Ar–C). The deformation (C–C) is observed at 1018 and δ(C–H) in the plane at 1069cm^{-1}. The broad absorption bands in the 876–1018 cm^{-1} range are due to γ(CCH). The δ(C–H) aromatic out the plane is observed at 770 cm^{-1}. The β(C–C) aromatic ring is experimentally observed at 584–701 cm^{-1}range. While the broad absorption bands in the 413–486 cm^{-1} range are due to δ(C–C–N–C).

Since the N–H modes are very weak in the Raman spectra. We can state that the band at 1200 cm^{-1} corresponds only to the pyridinium ring vibrations.

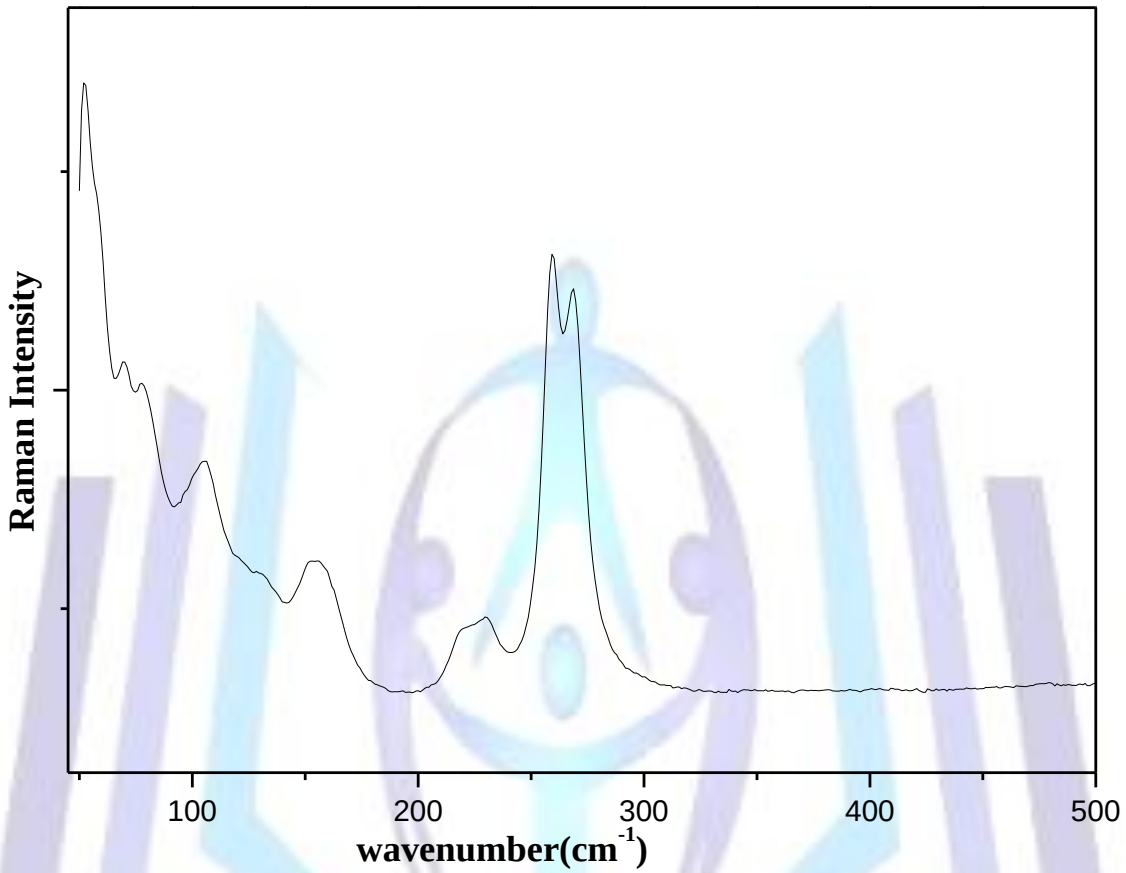

Fig 5: Raman spectra of $[C_8H_{12}N]_2Bi_2Cl_{10}$ in the range 50–500 cm^{-1}

ISSN 2321-807X

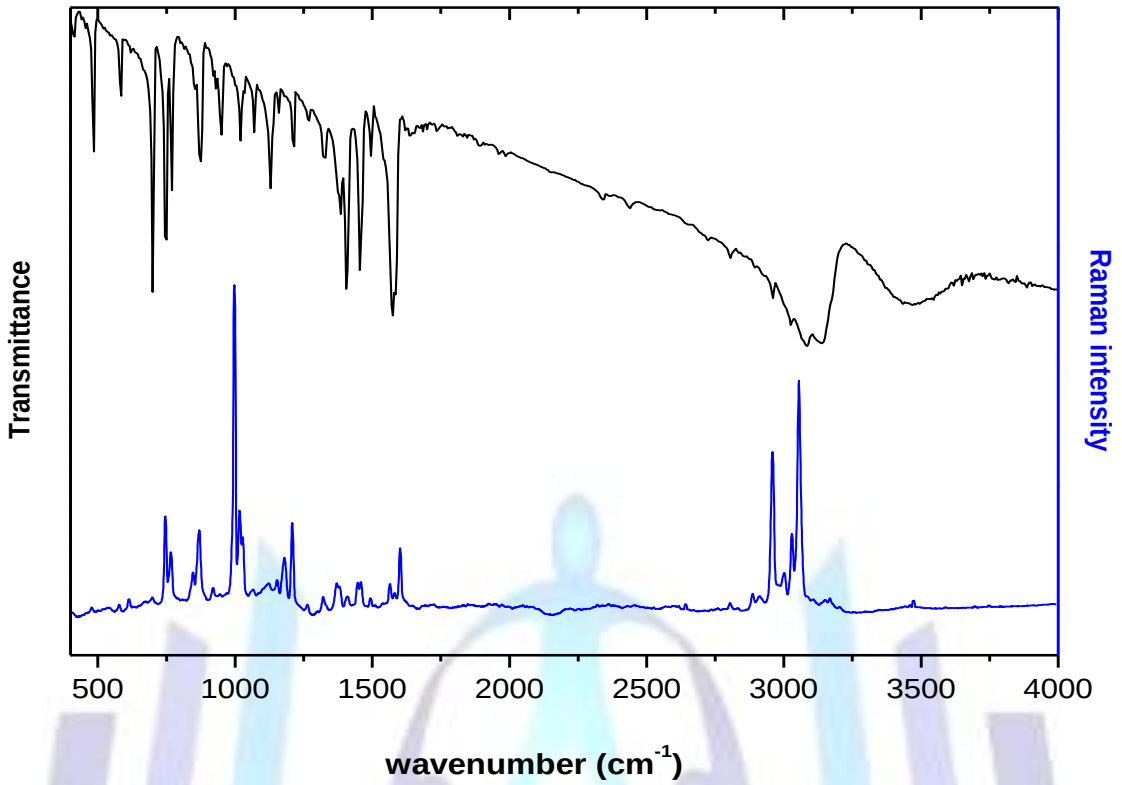

Fig 6: Superposition of IR and Raman spectra at the room temperature of $[C_8H_{12}N]_2BiCl_5$.

Table 4. Assignments of the IR wavenumbers in the range 400–4000 cm^{-1} and Raman in the range 50–4000 cm^{-1} for $[C_8H_{12}N]_2BiCl5$.

FT–IR	FT–Raman	Assignment
–	3473	
3462	–	ν(N–H) secondary
–	3460	
*v*NH … Cl –	3444	
–	3204	
–	3170	
–	3151	
3134	–	$\nu_a(NH_2^+)$, ν_a(C–H) aromatic
–	3106	
–	3088	$\nu_s(NH_2^+)$, ν_s(C–H) aromatic
3081	–	
–	3052	
–	3031	
3020	–	
–	3005	
–	2996	
–	2961	$\nu(CH_2)$

	2958	–	
	–	2914	
	–	2885	
	2808	–	
	–	2803	
Overtones	2719	–	ν(CH3)
	–	2642	
	–	1602	ν(C=C)
	2436	–	δ(NH2+)
	2339	–	
	–	1581	ν(C=C)
δNH … Cl	1577	–	
	–	1561	
	1497	–	
	–	1495	
	–	1459	
	1456	–	δ(CH3), δ(NH)
	–	1448	
	–	1410	δ(CH2), ν(C–H) aromatic
	1405	–	
	–	1403	
	–	1384	ω(CH2), δ(C–H)
	1383	–	
	–	1372	
	1325	–	
	–	1322	τ(CH2)
	1267	–	
	–	1266	λ(Ar–C)
	1212	–	
	–	1209	
	–	1179	δ(C–N)
	–	1172	
	1161	–	
	–	1156	
	1132	–	
	1069	–	δ(C–H) in plane
	–	1030	δ(C–C)
	–	1019	

	1018	–
	–	997
γ (CH)	949	–
	931	–
	–	920
	876	–
	–	870
	–	863
	–	846
	–	837
	770	–
	–	769
	–	759
	–	746
	745	–
	701	–
	621	–
	–	614
	584	–
	486	–
	456	–
	437	–
	413	–
	–	269
	–	260
	–	230
	–	218
	–	157
	–	152
	–	106
	–	78
	–	70
	–	57

γ(CCH)

δ(C–H) aromatic ring out of plane

φ(CH_2)

φ(NH_2)

δ(C–H) aromatic ring out of plane

β(C–C) aromatic ring

δ(C–C–N–C)

ν_a(Bi–Cl)

ν_s(Bi–Cl)

δ(Cl–Bi–Cl)

Bending mode

Lattice modes

Conclusion

Halogenobismuthate (III) has been prepared and studied by X-ray structure differential scanning calorimetry (DSC) and vibrational studies.

1. The atomic arrangement can be described as an alternation of organic and inorganic layers. The anionic layer is built up of octahedral $[Bi_2Cl_{10}]^{-4}$. The organic layers are arranged in sandwich between the anionic ones. The crystal packing is governed by means of the ionic N–H---Cl hydrogen bonds, forming a three dimensional network. The nature of the distortion of the inorganic polyhedra has been studied and can be attributed to the stereo activity of the Bi(III) lone electron pair.
2. DSC studies reveal the existence of phase transition at 407 K from phase I to phase II, which correspond probably to a clearly of first-order type.
3. The vibrational properties of this structure were studied by Raman scattering and infrared spectroscopy in the 4000–400 cm^{-1} frequency region.

ACKNOWLEDGEMENTS

This work was supported by the Minister Education and Research of Tunisia.

REFERENCES

[1] D.B. Mitzi, Prog. Inorg. Chem. 48 (1999) 1-121.

[2] G.C. Papavassiliou, Prog. Solid State Chem. 25 (3–4) (1997) 125.270

[3] M. Era, S. Morimoto, T. Tsutsui, S. Saito, Appl. Phys. Lett. 65 (6) (1994) 676-678.

[4] M. Wojtas, R. Jakubas, Z. Ciunik, W. Medycki, J. Solid State Chem. 177 (4-5) (2004) 1575-1584.

[5] G. Bator, Th. Zeegers-Huyskens, R. Jakubas, J. Zaleski, J. Mol. Struct. 570 (1) (2001) 61-74.

[6] B. Kulicka, T. Lis, V. Kinzhybalo, R. Jakubas, A. Piecha, Polyhedron 29 (8) (2010) 2014-2022.

[7] H. Eickmeier, B. Jaschinski, A. Hepp, J. Nuss, H. Reuter, R. Blachnik, Z Naturforsch Teil B 54 (3) (1999) 305-313.

[8] R. Jakubas, Solid State Commun. 69 (3) (1989) 267-269.

[9] J. Lefebvre, P. Carpentier, R. Jakubas, Acta Crystallogr. B 51 (2) (1995) 167-174.

[10] J. Jó´ zków, G. Bator, R. Jakubas, A. Pietraszko, J. Chem. Phys. 114 (16) (2001) 7239-7246.

[11] B. Kulicka, V. Kinzhybalo, R. Jakubas, Z. Ciunik, J. Baran, W. Medycki, J. Phys. 18 (22) (2006) 5087-5104.

[12] JM. Ryan, Z. Xu, Inorg. Chem. 43 (14) (2004) 4106-4108.

[13] D.B. Mitzi, Inorg. Chem. 39 (26) (2000) 6107-6113.

[14] S. Chaabouni, A. Hadrich, F. Romain, A.B. Salah, Solid State Sci. 5 (7) (2003) 1041-1046.

[15] K. Yamada, T. Tsuda, C. Holst, T. Okuda, H. Ehrenberg, I. Svoboda, H. Krane, H. Fuess, Bull. Chem. Soc. Jpn. 74 (1) (2001) 77-83.

[16] R. Jakubas, Z. Ciunik, G. Bator, Phys. Rev. B 67 (2) (2003) 241031. art. no. 024103.

[17] R. Jakubas, L. Sobczyk, Phase Transit. 20 (3-4) (1990) 163-193.

[18] V. Varma, R. Bhattacharjee, H.N. Vasan, C.N.R. Rao, Spectrochim. Acta A 48 (11– 12) (1992) 1631-1646.

[19] L. Sobczyk, R. Jakubas, J. Zaleski, Polish J. Chem. 71 (3) (1997) 265-300. and references cited therein.

[28] S. Chaabouni, S. Kamoun, J. Jaud, J. Chem. Crystallogr. 28 (3) (1998) 209-212.

[29] G.M. Sheldrick, SHELXS-86 (1990).

[30] X. Wang, F. Liebau, Acta Crystallogr. B 52 (1) (1996) 7-15.

[31] J. Zaleski, A. Pietraszko, Acta Crystallogr. B 52/2 (1996) 287-295.

[32] B. Kulicka, R. Jakubas, Z. Ciunik, Solid State Sci. 8 (10) (2006) 1229-1236.

[33] G.C. Pimental et, A.L. Mc Clellan, The Hydrogen Bond, Freeman, San Fransisco,1971.

[34] T. Barrowcliffe, I.R. Beattie, P. Day, K. Livingston, J. Chem. Soc. A (1967) 1810-1812.

[35] F. Zouari, A. Ben Salah, phase transitions. 78 (2005) 317-328.

[36] C. Hrizi, A. Samet, Y. Abid, S. Chaabouni, M. Fliyou, A. Koumina, J. Mol. Struct. 992 (2011) 96-101.

[37] B. Kulicka, R. Jakubas, A. Pietraszko, G. Bator, J. Baran. Solid State Sci. 6(11) (2004) 1273-1286.

[38] B. Bednarska-Bolek, J. Zaleski, G. Bator, R. Jakubas, J. Phys. Chem. Solids 61 (2000) 1249-1261.